ISSN 1063-7826, Semiconductors, 2018, Vol. 52, No. 9, pp. 1104–1109. © Pleiades Publishing, Ltd., 2018.
Original Russian Text © R.K. Yafarov, 2018, published in Fizika i Tekhnika Poluprovodnikov, 2018, Vol. 52, No. 9, pp. 980–985.

SURFACES, INTERFACES, AND THIN FILMS

Effect of High-Dose Carbon Implantation on the Phase Composition, Morphology, and Field-Emission Properties of Silicon Crystals

R. K. Yafarov

Kotel'nikov Institute of Radio Engineering and Electronics, Saratov Branch, Russian Academy of Sciences, Saratov, 410019 Russia

e-mail: pirpc@yandex.ru

Submitted October 2, 2017; accepted for publication October 18, 2017

Abstract—The study of high-dose carbon-ion implantation without post-process annealing reveals significant modification of the morphology, surface-layer phase composition, and field-emission properties of silicon wafers. The effect of the electrical conductivity type on the evolution of the silicon-crystal surface morphology, upon a variation in the irradiation dose, and a high content of diamond-like phases in the region of microprotrusions at the maximum dose regardless of the electrical conductivity type are found. It is demonstrated that the high-dose implantation of carbon in silicon wafers with a pre-structured surface increases the maximum density of field-emission currents by more than two orders of magnitude.

DOI: 10.1134/S1063782618090245

1. INTRODUCTION

Crystal silicon is one of the most attractive materials for field electron sources used as active elements of vacuum microelectronics. This is mainly due to its highly developed technology and the luminescence properties of nanocrystalline silicon, which give grounds to expect the creation of superhigh-speed radiation-resistant silicon chips with optical coupling.

The drawbacks of silicon-based field electron sources are their high sensitivity to the surface state and low field-emission current density ranging, as a rule, within 50–150 $\mu A/cm^2$ [1, 2]. Such current densities satisfy the requirements for purely silicon field-emission cathodes used in field-emission displays (FEDs) [3]. However, this is insufficient for designing, for example, vacuum field-effect transistors with a high output power.

A research direction promising for the creation of high-current field electron sources is the fabrication of cathode matrices by implanting carbon ions in silicon substrates [4]. Irradiation with ions with energies modifying the substrate properties at different depths makes it possible to flexibly control the phase-composition distribution in a substrate and, consequently, the electrical properties. In addition, choosing an appropriate type of ions, one can employ an additional way of modification associated with the chemical interaction between implanted ions and the emitter material.

The aim of this work is to investigate the effect of high-dose ion-beam carbon processing of the surface regions of Si(100) wafers on their structural and phase composition, morphology, and field-emission properties.

2. EXPERIMENTAL

Carbon-ion implantation was performed on a facility with a Raduga-3M pulsed ion source operating at an accelerating voltage of 80 kV and doses ranging from 1×10^{17} to 1×10^{18} cm^{-2}. Silicon wafers of different conductivity types (KES (0.01–0.02), KDB (0.01–0.02), KEF-4.5, and KDB-7.5) were used. The surface of silicon was structured by depositing island carbon masks in a microwave ethanol-vapor plasma onto silicon crystals with a natural-oxide coating with subsequent highly anisotropic plasma-chemical etching in Khladon-14 plasma using the technique described in [5]. The morphology and phase composition of the ion-implanted silicon wafers were analyzed by atomic force microscopy and confocal Raman spectroscopy. The confocal Raman spectroscopy investigations were carried out using an NT-MDT Integra Spectra probe nanolaboratory. The Raman spectra were recorded in the frequency range of 150–3000 cm^{-1} with a resolution of 1.7 cm^{-1} using a cooled CCD camera under excitation by a solid-state laser ($\lambda = 473$ nm). Radiation was focused by a 100× objective lens with a numerical aperture NA = 0.95 ensuring a laser spot size of ~0.6 μm at the specified wavelength for obtaining a sufficient degree of locality when studying surface-relief features. The P4-SPM-MDT scanning atomic force microscope probes were standard CSG10 pyramidal silicon cantilevers with a curvature radius of 10 nm and a rigidity of 0.1 N/m. The

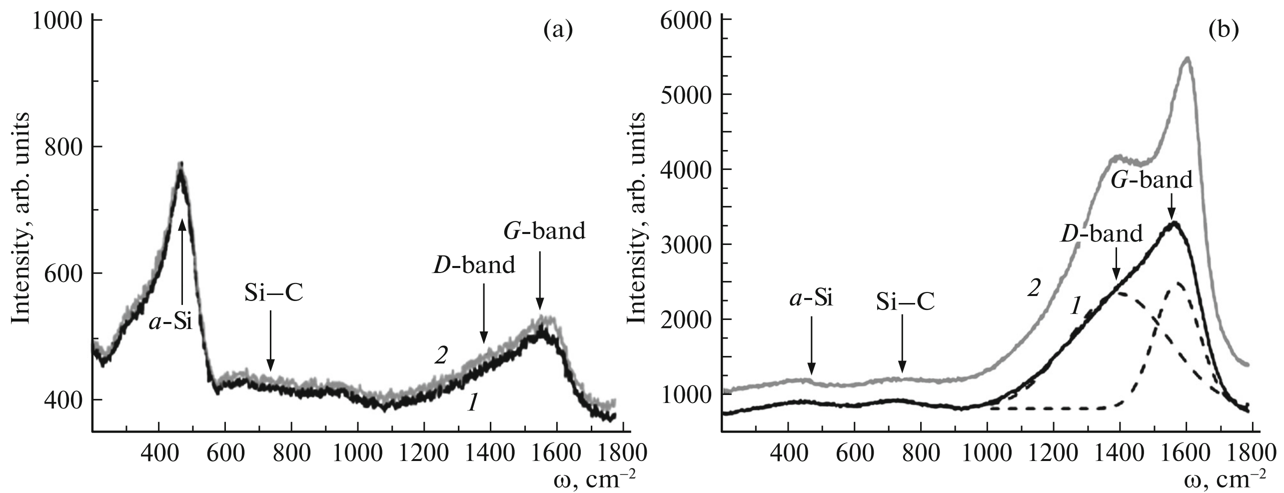

Fig. 1. Raman scattering spectra of the silicon samples irradiated with C^+ ions at doses of (a) 1×10^{17} cm^{-2} and (b) 1×10^{18} cm^{-2} at 80 kV. Different curves correspond to different surface points: (*1*) beyond the protrusion and (*2*) inside it. Dashed lines show the decomposition of one experimental spectrum into Gaussian lines.

field-emission properties were investigated in high vacuum (a residual pressure of 10^{-6} Pa) for a diode structure capable of changing the interelectrode distance to 1 μm. The working surface diameter of an anode fabricated from MPG-6 carbon material was 3 mm.

Figure 1 shows the Raman scattering spectra of the silicon samples irradiated with C^+ ions in doses of 5×10^{17} and 1×10^{18} cm^{-2} at 80 kV. It can be seen that irradiation, as expected, leads to amorphization of the silicon surface layer (scattering bands corresponding to the amorphous Si layer arise). The presence of implanted carbon is reflected in the broad bands at 1350 and 1585 cm^{-1}; the intensity of these bands increases with the C^+ dose. The positions of the lines are in good agreement with the positions of the known *G* and *D* Raman scattering bands on the sp^2 and sp^3 bonds in amorphous carbon [6]. Some carbon atoms bind to silicon and give a broad scattering band at 740 cm^{-1}, the parameters of which do not significantly depend on the C^+ dose. As the implanted ion dose increases, the amorphous-silicon fraction decreases and the carbon-phase fraction increases. The carbon-containing phase composition changes most intensively in the protrusions on the silicon surface.

To obtain a quantitative carbon-dose dependence of the sp^3 and sp^2 bonds, the carbon Raman scattering band was decomposed into the Gaussian components corresponding to the *G* and *D* lines. The ratio between the intensities of the *G* and *D* bands, which gives an idea about the relative content of the diamond-like and graphite phases, was determined from the ratio between the integrated intensities of these bands (Table 1). It can be seen that the ratio between the diamond-like and graphite phases forming in the crystal silicon surface region depends on both the irradiation dose and morphological characteristics of the surface. With increasing dose, a trend toward the relative growth of the *D* Raman scattering line is observed, which is caused by the formation of a diamond-like carbon phase. The changes are especially pronounced inside silicon surface protrusions, where the diamond-like phase fraction increases by about 20% relative to the case of a smooth surface. In the smooth areas on the implanted silicon surface, there is no noticeable dose dependence of the change in the ratio between the *D* and *G* lines (the diamond-like phase fraction beyond the microprotrusions is 60–63%).

Figures 2–5 show the dependences of the morphological and field-emission characteristics on the dose of irradiation with carbon ions with an energy of 80 keV obtained in the continuous measuring mode on smooth and pre-structured KES (0.01–0.02) and KDB (0.01–0.02) silicon wafers. One can see in Fig. 2a that with increasing irradiation dose the height of protrusions on the initially smooth *p*-type silicon wafers increases, while on the pre-structured surfaces it rapidly decreases. At an irradiation dose of 1×10^{18} cm^{-2}, the morphological parameters of the wafers with the initially structured and smooth surfaces become almost identical.

In the case of *n*-type silicon wafers, the effect of ion irradiation on the surface morphology is significantly different. It can be seen in Fig. 4a that for the wafers with an unstructured surface, the protrusion height increases with irradiation dose, as in the *p*-type silicon wafers. However, for *n*-type silicon, this increase is several times greater. With an increase in the irradiation dose, the height of protrusions on the pre-structured *n*-type silicon surface remains almost invariable, while for the *p*-type wafers it rapidly drops.

Table 1. Relative contribution of the G and D bands of the Raman scattering spectra in the range of 1000–1700 cm^{-1} for the silicon samples irradiated with C^+ ions at different doses

C^+ dose, cm^{-2}	Analyzed region	Relative contribution of the G band, %	Relative contribution of the D band, %
5×10^{17}	Beyond a protrusion	39	62
	In a protrusion	40	60
1×10^{18}	Beyond a protrusion	37–38	62–63
	In a protrusion	18–19	81–82

The threshold of the field-emission strength on the pre-structured p-type silicon surface slightly increases with increasing radiation dose; at all irradiation doses, it is smaller than upon emission from the initially smooth wafers (Fig. 3a). On the contrary, in the n-type silicon wafers it decreases fairly fast with increasing radiation dose (Fig. 5a).

The irradiation-dose dependences of the maximum field-emission current densities and densities of protrusions on the smooth and surface-structured Si(100) wafers of both conductivity types are qualitatively similar. The analogous high-dose carbon-ion implantation of silicon wafers of both conductivity types with pre-structured surfaces leads to the almost identical morphological characteristics of the surfaces ($h \approx$ 7–10 nm, $\rho \approx (3–5) \times 10^{10}$ cm^{-2}), but in the n-type silicon wafers it appears more effective. At an irradiation dose of 1×10^{18} cm^{-2}, the maximum field-emission current density in the n-type silicon wafers is higher than in the p-type silicon ones by 25–30%.

3. RESULTS AND DISCUSSION

The calculated distribution and ion concentration (defect) profiles under the irradiation of silicon wafers with a smooth surface show that the ions implanted using the chosen implantation regimes (without regard for possible redistribution) should be concentrated in the surface layer at a depth of ~400 nm [7]. At extreme doses of 1×10^{17} and 1×10^{18} cm^{-2}, the carbon atom densities of ~6.4×10^{21} and ~6.4×10^{22} cm^{-3} are attained in the profile maximum without regard for sputtering. Such dopant concentrations are sufficient to form carbon nanophases in silicon, including stoichiometric silicon carbide SiC [8] (the atomic concentration in the Si crystal is 5×10^{22} cm^{-3}). The estimates made when choosing the silicon-wafer irradiation doses are consistent with the experimental results. They show that, as expected, the phase composition of implanted C^+ silicon layers is independent of the semiconductor electrical conductivity type and includes four amorphous phases: a-Si (scattering band with the maximum at 480 cm^{-1}), silicon carbide (scattering band at 740 cm^{-1}), and diamond-like (D Raman scattering band at 1585 cm^{-1} on the sp^3 bonds in a-C) and graphite-like carbon (G Raman scattering band at 1350 cm^{-1} on the sp^2 bonds in a-C). The SiC peak is significantly lower than the carbon-phase peaks. A significant amount of this phase arises at a dose of 5×10^{17} cm^{-2}, and, with an increase in the dose to 1×10^{18} cm^{-2}, its relative contribution decreases. The latter can be interpreted as the partial decomposition of SiC. The most significant result is the growth of the

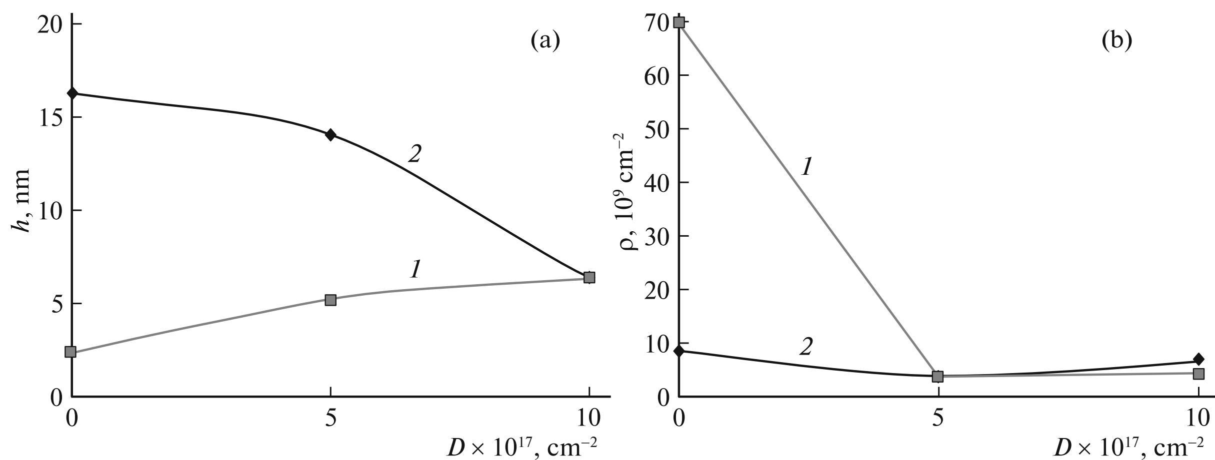

Fig. 2. Irradiation-dose dependences of (a) the height and (b) density of protrusions on (*1*) the initial and (*2*) surface-structured p-Si(100) wafers.

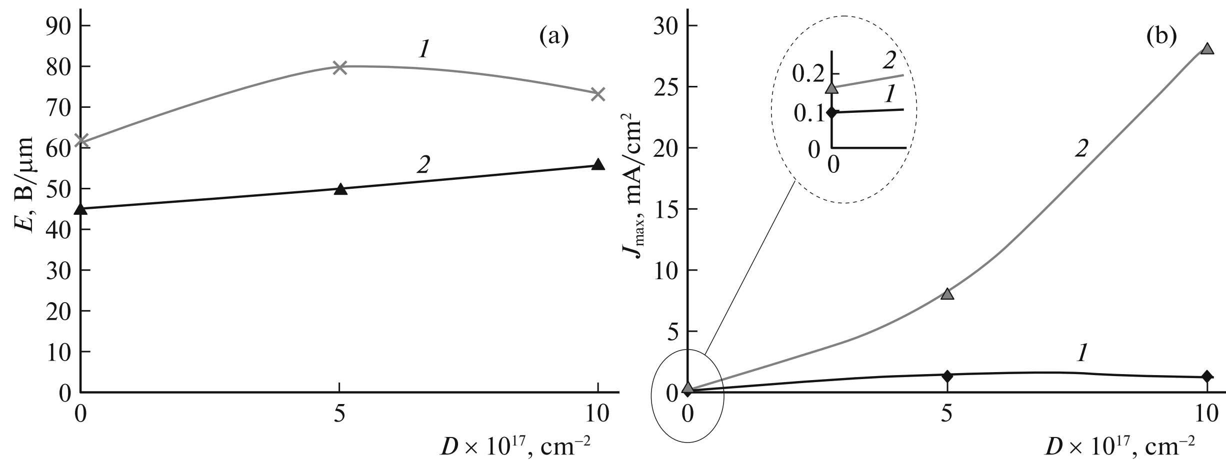

Fig. 3. Carbon-ion irradiation dose dependences of (a) the thresholds and (b) maximum electron field-emission current densities for (*1*) the initial (smooth) and (*2*) surface-structured *p*-Si(100) wafers. Inset: maximum field-emission current density without carbon implantation.

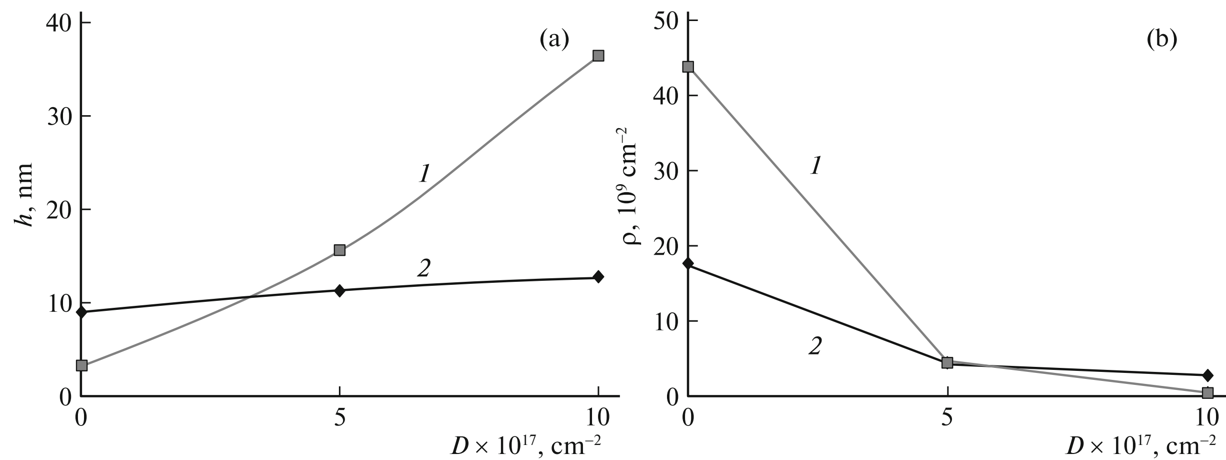

Fig. 4. Carbon-ion irradiation dose dependences of (a) the heights (a) and (b) densities of protrusions on (*1*) the initial and (*2*) surface-structured *n*-Si(100) wafers.

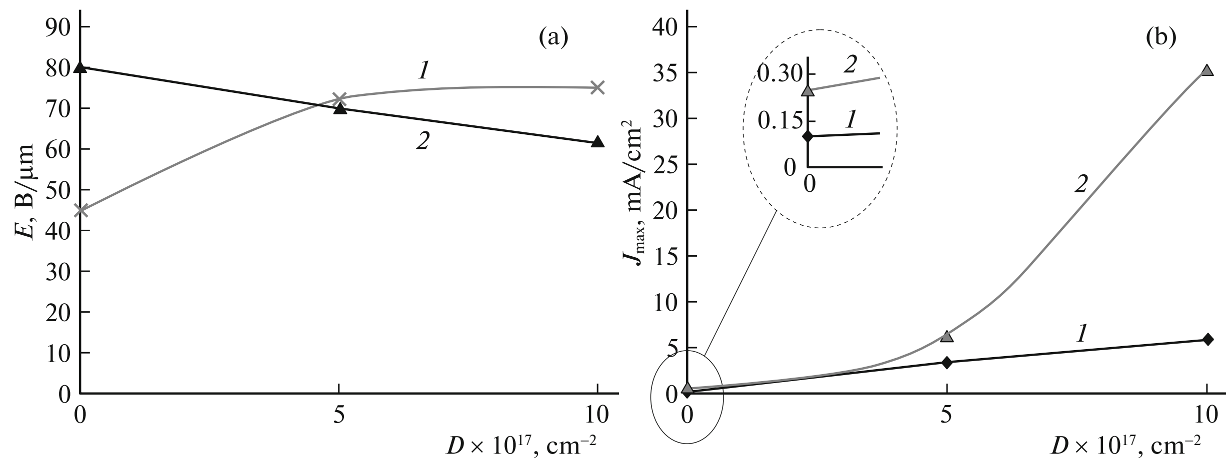

Fig. 5. Carbon-ion irradiation dose dependences of (a) the thresholds and (b) maximum electron field-emission current densities on (*1*) the initial and (*2*) surface-structured *n*-Si(100) wafers. Inset: maximum density of the field-emission current without carbon implantation.

diamond-like phase fraction in silicon microprotrusions at a dose of 1×10^{18} cm^{-2}, which is over 80%. In this case, the intensities of the *D* and *G* lines grow, which is indicative of structural ordering of the corresponding phases.

According to modern concepts, the dominant formation of diamond nanophases in microprotrusions under high-dose carbon ion implantation originates from the instability of the amorphized flat silicon surface layer under high-intensity ion processing [9]. Minimization of the free surface energy of the system leads to an increase in the relative amount of the diamond-like phase, the surface energy of which is higher than that of the graphite phase. This is facilitated by a reduction in the heat sinks and thermomechanical stresses induced by the temperature gradient in protrusions relative to a smooth surface. As a result, the maximum temperature in local heat peaks arising in the tracks of implanted carbon ions increases. These two factors contribute to the formation of a diamond-like phase [10].

The evolution of the silicon-wafer surface morphology upon a variation in the dose of implanted carbon ions corresponds to concepts in which the relief formation under ion irradiation is attributed to self-assembly directed to attaining the minimum free surface energy, rather than development of the initial morphologies due to the sputtering of surface atoms [9]. Such morphological characteristics are related to the ion-irradiation parameters and composition of the forming surface phases. Therefore, for example, at high irradiation doses, the surface densities and height of protrusions formed on *p*-type silicon wafers with different initial morphologies become almost identical.

The different characters of the variation in the morphological parameters with the dose of irradiation with C^+ ions for silicon wafers with different conductivity types is most likely due to the effect of the impurity, which determines the semiconductor electrical-conductivity type. At the same kinetic energy, dose, and current density of carbon ions bombarding the substrate, due to a lower coefficient of sputtering of phosphorus atoms caused by a large difference between their masses, as well as better neutralization of the implanted positive carbon ions in the electronic semiconductor, the protrusions on *n*-type silicon are higher than upon the sputtering of *p*-type silicon. In the latter case, the accommodation coefficient, i.e., the efficiency of energy transfer from carbon leads to more uniform sputtering of an unstructured silicon surface and fast sputtering of the protrusion tops for a pre-structured surface (Fig. 4a).

Without ion irradiation, the lower threshold of the field-emission onset for the pre-structured *p*-type silicon wafer surface is determined, according to the Fowler and Nordheim concepts, by a large field amplification coefficient on high protrusions (Figs. 3a and 5a). With an increase in the irradiation dose to 1×10^{18} cm^{-2}, the height of protrusions on structured *p*-type silicon decreases by a factor of more than three. In this case, however, the field-emission thresholds increase rather than decrease. Simultaneously, an increase in the maximum field-emission current densities by more than two orders of magnitude as compared with analogous unirradiated wafers is observed.

For the *n*-type silicon wafers with the initially structured surface, the highest field-emission threshold is implemented in the absence of carbon irradiation. As the irradiation dose increases to 1×10^{18} cm^{-2}, the protrusion height remains almost invariable. In this case, however, the field-emission thresholds significantly (by about 25%) decrease and, as in the *p*-type silicon wafers, the maximum field-emission current densities nonlinearly increase. In the *n*-type silicon wafers, the height of protrusions on the unstructured surface, which form at an ion irradiation dose of 1×10^{18} cm^{-2}, exceed the height of protrusions on the pre-structured surface by a factor of more than three (Fig. 4a). Nevertheless, the thresholds of field-emission onset in silicon wafers with a pre-structured surface are lower and the maximum field-emission current densities, as in the case of high-dose irradiation of *p*-type silicon crystals, exceed the maximum current densities in the analogous unirradiated wafers by more than two orders of magnitude (Fig. 5). These relations between the morphological parameters and field-emission properties of the silicon crystals cannot be interpreted within the framework of the Fowler and Nordheim representations and indicate a qualitative change in their structure under high-dose carbon ion implantation. Obviously, these changes are caused by structural and phase transformations, in particular, the formation of diamond-like nanophases in the surface region of silicon crystals, which facilitate lowering of the field-emission thresholds and increase in the maximum field-emission current densities [11]. According to the results of structural and phase investigations under high-dose irradiation, their formation, as well as nonlinear growth of the maximum field-emission current density, is independent of the type of conductivity of a silicon crystal.

4. CONCLUSIONS

High-dose carbon implantation can lead to the double effect of improving the efficiency of field emission from silicon cathode matrices. Firstly, this is spontaneous structuring of the surface layer microrelief due to sputtering of the target surface atoms by accelerated carbon ions. At identical ion-irradiation regimes, the surface microrelief, which determines the possibility of amplifying the field on the emitting protrusions, is determined by the type of impurity, which characterizes the type of electrical conductivity of a semiconductor crystal. Secondly, this is the change in the phase composition of the surface silicon layers,

which is independent of the electrical conductivity type. This is caused by an increase in the relative contents of graphite- and diamond-like carbon at the expense of the *a*-Si and *a*-SiC phases with an increase in the irradiation dose, as well as by a variation in the ratio between the sp^3- and sp^2-bond concentrations in favor of the former with traces of crystallization in the surface relief microprotrusions.

The specific features of the evolution of the morphological characteristics of silicon wafers with different electrical conductivity types and their surface pretreatment upon a variation in the implanted carbon ion dose were established. The change in the heights and surface densities of protrusions with the irradiation dose is caused by rearrangement of the initial silicon surface reliefs under the action of ion sputtering.

Under high-dose carbon irradiation, the surface density of microprotrusions on the silicon wafers is independent of the initial morphology and amounts to $(3–5) \times 10^9$ cm^{-2}. However, the initial morphology of the silicon wafers strongly affects modification of the phase composition of the surface layer and their field-emission properties. Thus, in *p*-type silicon wafers with the initially structured surface, the maximum current density as compared with the silicon crystals with the initially unstructured surface, irradiated with carbon ions at the same dose, increases by more than an order of magnitude and, as compared to the unirradiated *p*-type silicon crystals, by more than two orders of magnitude. Similar changes in the field-emission properties are observed upon high-dose carbon implantation of the *n*-type silicon wafers with the prestructured surface.

ACKNOWLEDGMENTS

This study was supported by the Russian Science Foundation, project no. 16-19-10033.

REFERENCES

1. L. F. Velásquez-García, S. Guerrera, Y. Niu, and A. I. Akinwande, IEEE Trans. Electron Dev. **58**, 1783 (2011).
2. Yu. B. Gulyaev, N. P. Aban'shin, B. I. Gorfinkel', S. P. Morev, A. F. Rezchikov, N. I. Sinitsyn, and A. N. Yakunin, Tech. Phys. Lett. **39**, 525 (2013).
3. Fei Zhao, Jian-hua Deng, Dan-dan Zhao, Ke-fan Chen, Guo-an Cheng, and Rui-ting Zheng, J. Nanosci. Nanotechnol. **10**, 1 (2010).
4. P. G. Bobovnikov, A. S. Ermakov, I. V. Matyushkin, S. N. Orlov, K. P. Svechkarev, N. A. Shelepin, A. N. Mikhailov, and A. I. Belov, Izv. Vyssh. Uchebn. Zaved., Elektron., No. 5 (103), 3 (2013).
5. R. K. Yafarov and V. Ya. Shanygin, Semiconductors **51**, 531 (2017).
6. X. L. Ding, Q. S. Li, and X. H. Kong, Phys. B (Amsterdam, Neth.) **404**, 1920 (2009).
7. S. M. Sze, *Physics of Semiconductor Devices* (Wiley, New York, 1981; Mir, Moscow, 1986), Vol. 1.
8. K. Kh. Nusupov, N. B. Beisenkhanov, I. V. Valitova, E. A. Dmitrieva, D. Zhumagaliuly, and E. A. Shilenko, Phys. Solid State **48**, 1255 (2006).
9. N. N. Gerasimenko and Yu. N. Parkhomenko, *Silicon is the Material of Nanotechnologies* (Tekhnosfera, Moscow, 2007) [in Russian].
10. *Diamonds in Electronics, Collection of Articles*, Ed. by V. B. Kvaskov (Energoatomizdat, Moscow, 1990) [in Russian].
11. R. K. Yafarov, Tech. Phys. **51**, 40 (2006).

Translated by E. Bondareva